J|A|C|S ARTICLES

Published on Web 03/16/2009

Activation Parameters for Heme−NO Binding in *Alcaligenes xylosoxidans* Cytochrome *c′*: The Putative Dinitrosyl Intermediate Forms via a Dissociative Mechanism

David A. Pixton,[‡] Christine A. Petersen,[‡] Alicja Franke,[⊥] Rudi van Eldik,*[,⊥] Elizabeth M. Garton,[‡] and Colin R. Andrew*[,‡]

Department of Chemistry and Biochemistry, Eastern Oregon University, One University Boulevard, La Grande, Oregon 97850-2899, and Department of Chemistry and Pharmacy, University of Erlangen-Nürnberg, Egerlandstrasse 1, 91058 Erlangen, Germany

Received December 8, 2008; E-mail: vaneldik@chemie.uni-erlangen.de; candrew@eou.edu

Abstract: The bacterial heme protein *Alcaligenes xylosoxidans* cytochrome *c′* (AXCP) forms a novel five-coordinate heme−nitrosyl (5c-NO) complex in which NO resides at the *proximal* heme face in place of the endogenous protein ligand. Intriguingly, AXCP shares NO-binding properties with the eukaryotic NO-sensor, soluble guanylate cyclase (sGC), including 5c-NO formation *via two NO-dependent reactions*. For both proteins, a model has been proposed in which NO binds to the vacant distal face to form a transient six-coordinate heme−nitrosyl (6c-NO) species, which then converts to a proximal 5c-NO complex via a putative dinitrosyl intermediate. To shed light on this novel reaction mechanism, activation parameters have been determined for distal and proximal NO-binding reactions in AXCP from the effect of temperature and hydrostatic pressure on rate constants. The unusually slow 6c-NO formation reaction has a near-zero entropy of activation and a positive volume of activation ($\Delta V^{\ddagger} = +14.1$ cm^3 mol^{-1}), consistent with a rate-determining step involving movement of the Leu 16 residue to allow NO binding to the crowded distal site. For the 6c-NO → 5c-NO conversion, the large positive entropy of activation ($\Delta S^{\ddagger} = +103$ J K^{-1} mol^{-1}) and volume of activation ($\Delta V^{\ddagger} = +24.1$ cm^3 mol^{-1}) suggest that the putative dinitrosyl intermediate forms via a dissociative mechanism in which the endogenous His ligand dissociates *prior to the attack* of the second NO molecule on the proximal heme face. These results have important implications for distal vs proximal NO binding in AXCP, as well as mechanisms of 5c-NO formation in heme proteins.

Introduction

Cytochromes *c′* are bacterial heme proteins that contain a pentacoordinate *c*-type heme within a four-α-helix bundle.[1,2] While cytochromes *c′* have been characterized for over 30 years, their physiological function is still unclear. The vacant distal coordination site points to a ligand-binding role, rather than the electron-transfer function typical of hexacoordinate *c*-type heme proteins such as mitochondrial cytochrome *c*. Electron paramagnetic resonance spectroscopy of whole cells has confirmed the presence of cytochromes *c′* as the ferrous−nitrosyl complex.[3,4] It has been proposed that cytochromes *c′* may protect bacteria from the toxicity of free nitric oxide (NO) in their environment[5−9] by acting either as a NO reductase or as a NO transporter to an auxiliary reductase system, although the molecular details of these proposed functions have yet to be confirmed. All cytochromes *c′* characterized to date are able to bind NO and CO but are unable to form stable complexes with O_2. X-ray crystal structures of various cytochromes *c′* show that the empty distal heme face is relatively buried and packed with hydrophobic residues including a Leu, Met, or Phe residue positioned over the Fe (see, for example, ref 2). In contrast, the proximal heme face is closer to the protein surface, with the His ligand exposed to solvent.

Particular interest surrounds the novel coordination chemistry of cytochrome *c′* from the denitrifier, *Alcaligenes xylosoxidans*. This protein, termed AXCP, exhibits the unprecedented coordination of exogenous ligands to either heme face (distal or proximal).[10,11] Crystal structures of AXCP show that CO forms a six-coordinate heme−carbonyl (6c-CO) complex on the distal heme face, whereas NO forms an unprecedented five-coordinate

[‡] Eastern Oregon University.
[⊥] University of Erlangen-Nürnberg.

(1) Ambler, R. P.; Bartsch, R. G.; Daniel, M.; Kamen, M. D.; McLellan, L.; Meyer, T. E.; Van Beeumen, J. *Proc. Natl. Acad. Sci. U.S.A.* **1981**, *78*, 6854–6857.
(2) Ramirez, L. M.; Axelrod, H. L.; Herron, S. R.; Rupp, B.; Allen, J. P.; Kantardjieff, K. A. *J. Chem. Crystallogr.* **2003**, *33*, 413–424.
(3) Yoshimura, T.; Iwasaki, H.; Shidara, S.; Suzuki, S.; Nakahara, A.; Matsubura, T. *J. Biochem.* **1988**, *103*, 1016–1019.
(4) Yoshimura, T.; Shidara, S.; Ozaki, T.; Kamada, H. *Arch. Microbiol.* **1993**, *160*, 498–500.
(5) Cross, R.; Aish, J.; Paston, S. J.; Poole, R. K.; Moir, J. W. B. *J. Bacteriol.* **2000**, *182*, 1442–1447.
(6) Cross, R.; Lloyd, D.; Poole, R. K.; Moir, J. W. B. *J. Bacteriol.* **2001**, *183*, 3050–3054.
(7) Anjum, M. F.; Stevanin, T. M.; Read, R. C.; Moir, J. W. B. *J. Bacteriol.* **2002**, *184*, 2987–2993.
(8) Mayburd, A. L.; Tan, Y.; Kassner, R. J. *Arch. Biochem. Biophys.* **2000**, *378*, 40–44.
(9) Choi, P. S.; Grigoryants, V. M.; Abruña, H. D.; Scholes, C. P.; Shapleigh, J. P. *J. Bacteriol.* **2005**, *187*, 4077–4085.
(10) Lawson, D. M.; Stevenson, C. E. M.; Andrew, C. R.; Eady, R. R. *EMBO J.* **2000**, *19*, 5661–5671.
(11) Lawson, D. M.; Stevenson, C. E. M.; Andrew, C. R.; George, S. J.; Eady, R. R. *Biochem. Soc. Trans.* **2003**, *31*, 553–557.

 10.1021/ja809587q CCC: $40.75

Scheme 1. Heme−NO Binding Mechanism in AXCP, Showing the Three Detectable Heme Species: (a) 5c-Fe^{2+}, (b) 6c-NO, and (c) 5c-NO, as Well as the Proposed Dinitrosyl Intermediate

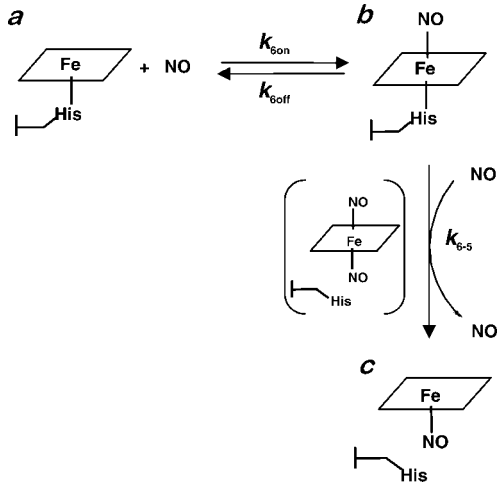

heme−nitrosyl (5c-NO) complex on the proximal heme face, replacing the endogenous His 120 ligand.[10] The ability of AXCP to use both of its heme faces to bind exogenous ligands represents a novel strategy for ligand discrimination by a heme protein.[12] Although the functional significance of distal vs proximal NO binding in AXCP is not yet known, it is possible that it helps modulate ligand interactions in the context of its proposed NO-binding role.

Indeed, ligand binding to both the distal and proximal heme faces of AXCP is a central feature of the proposed mechanism for 5c-NO formation. Previous kinetic studies of NO binding to AXCP have shown that the proximal 5c-NO complex is formed via a transient six-coordinate heme−nitrosyl (6c-NO) species.[13−15] Significantly, the rates of formation of the 6c-NO precursor and the subsequent 6c-NO → 5c-NO conversion are both first-order with respect to NO concentration. A model has been proposed in which NO first binds to the vacant distal face of the ferrous heme to form a 6c-NO intermediate, which then converts to the proximal 5c-NO product via a putative dinitrosyl intermediate (Scheme 1).[11,14] Although a dinitrosyl species has yet to be identified in any heme protein, its existence in AXCP is postulated from the NO-dependence of its 6c-NO → 5c-NO conversion rate,[11,14] together with the proximal heme−NO coordination of the 5c-NO−AXCP crystal structure. Computational studies confirm that a heme−dinitrosyl intermediate is a plausible species in the proximal 5c-NO formation mechanism.[16,17]

Intriguingly, NO-dependent 6c-NO → 5c-NO kinetics are also observed for the eukaryotic heme-based NO sensor, soluble guanylate cyclase (sGC),[18,19] an enzyme that is part of the NO/cGMP signaling cascade in the cardiovascular and central nervous systems. While a crystal structure of the sGC heme domain has yet to be reported, proximal heme−NO binding (via a transient dinitrosyl species) is one of the models proposed to account for the observation of a second NO-binding reaction.[20−22] In this case, the interconversion between distal and proximal heme−NO coordination (via a dinitrosyl heme intermediate) could be relevant to ligand discrimination and regulation of sGC activity.[20−22]

Important questions regarding the mechanism of proximal heme−NO formation include (i) what factors govern distal vs proximal NO coordination, and (ii) how is the putative dinitrosyl intermediate formed? Detailed information on the mechanisms of ligand-binding reactions can be obtained by measuring activation parameters, including the entropy of activation ($\Delta S^{\ddagger}$), enthalpy of activation ($\Delta H^{\ddagger}$), and volume of activation ($\Delta V^{\ddagger}$). These activation parameters describe changes in the properties of reactants on going from the ground state to the transition state and, therefore, relate to the elementary step that is rate-determining (in heme proteins this step may involve formation/breakage of Fe−ligand bonds or conformational changes in the protein matrix). Values of $\Delta S^{\ddagger}$ and $\Delta H^{\ddagger}$ can be calculated from the temperature-dependence of rate constants, while $\Delta V^{\ddagger}$ can be obtained by measuring rate constants as a function of hydrostatic pressure. In the present study, temperature- and pressure-dependent stopped-flow kinetic measurements were carried out on the reaction of NO with ferrous AXCP to probe the mechanisms of distal and proximal heme−NO binding. Overall, the data suggest that steric hindrance is an important influence of distal heme−NO interactions in AXCP, while the switch from distal to proximal NO binding is governed by the rate of dinitrosyl formation, which requires the release of the proximal His ligand to form a distal 5c-NO intermediate, followed by rapid reaction of a second NO with the solvent-exposed heme.

Methods

Preparation of Solutions. Samples of AXCP were a gift from Dr. Robert Eady. The protein was isolated and purified as previously described.[23,24] All solutions used for kinetic measurements were prepared anaerobically in 50 mM CHES buffer (pH 8.9) containing 0.10 M NaCl to match the conditions of previous studies. NO gas (Aldrich) was bubbled through 0.1 M KOH solution to remove higher oxides of nitrogen. Stock solutions of NO were prepared by equilibrating a 1:5 mixture of NO and N_2 gas with buffer at 25.0 °C to give a concentration of 0.38 mM. Dilutions of the NO stock solution were made with anaerobic buffer inside a gastight syringe, with the headspace removed to avoid gas equilibration. Ferrous AXCP was prepared by the reduction of ferric protein with a 40-fold excess of sodium ascorbate. The presence of ascorbate in solution did not affect the reaction kinetics.

Stopped-Flow Measurements. Temperature-dependent kinetic measurements of the reaction of ferrous AXCP with NO were carried out over the range 10.0−30.0 °C using an Applied Photophysics SX.18MV-R stopped-flow spectrophotometer (dead time ~1 ms) housed within an anaerobic glovebox (Coy Laboratory Products Inc.). Solutions of ferrous protein were rapidly mixed with equal volumes of NO-containing buffer, and the reactions were

(12) Andrew, C. R.; Green, E. L.; Lawson, D. M.; Eady, R. R. *Biochemistry* **2001**, *40*, 4115–4122.
(13) George, S. J.; Andrew, C. R.; Lawson, D. M.; Thorneley, R. N. F.; Eady, R. R. *J. Am. Chem. Soc.* **2001**, *123*, 9683–9684.
(14) Andrew, C. R.; George, S. J.; Lawson, D. M.; Eady, R. R. *Biochemistry* **2002**, *41*, 2353–2360.
(15) Andrew, C. R.; Rodgers, K. R.; Eady, R. R. *J. Am. Chem. Soc.* **2003**, *125*, 9548–9549.
(16) Tangen, E.; Conradie, J.; Svadberg, A.; Ghosh, A. *J. Inorg. Biochem.* **2005**, *99*, 55–59.
(17) Martí, M. A.; Capece, L.; Crespo, A.; Doctorovich, F.; Estrin, D. A. *J. Am. Chem. Soc.* **2005**, *127*, 7721–7728.
(18) Zhao, Y.; Brandish, P. E.; Ballou, D. P.; Marletta, M. A. *Proc. Natl. Acad. Sci. U.S.A.* **1999**, *96*, 14753–14758.
(19) Ballou, D. P.; Zhao, Y.; Brandish, P. E.; Marletta, M. A. *Proc. Natl. Acad. Sci. U.S.A.* **2002**, *99*, 12097–12101.
(20) Cary, S. P.; Winger, J. A.; Marletta, M. A. *Proc. Natl. Acad. Sci. U.S.A.* **2005**, *102*, 13604–13609.
(21) Russwurm, M.; Koesling, D. *EMBO J.* **2004**, *23*, 4443–4450.
(22) Poulos, T. L. *Curr. Opin. Struct. Biol.* **2006**, *16*, 736–743.
(23) Ambler, R. P. *Biochem. J.* **1973**, *1345*, 751–758.
(24) Norris, G. E.; Anderson, B. F.; Baker, E. N.; Rumball, S. V. *J. Mol. Biol.* **1979**, *135*, 309–312.

monitored with monochromatic light (416 nm) using a photomultiplier detector. Concentrations of dissolved NO (40−190 μM after mixing) were maintained in at least 10-fold excess over the heme-binding sites (~3 μM after mixing) to ensure pseudo-first-order conditions. Pseudo-first-order rate constants were determined by fitting time courses to a two-exponential function and are the average of 3−5 separate kinetic runs. Time-resolved absorption spectra were obtained using a diode-array detector capable of recording absorption spectra (300−700 nm) with 1.28-ms temporal resolution. Global analysis of multiwavelength kinetic data was carried out using the Pro Kineticist software package.

High-pressure stopped-flow experiments were performed at pressures up to 130 MPa on a custom-built instrument described previously.[25,26] Kinetic traces were recorded on an IBM-compatible computer and analyzed with the OLIS KINFIT (Bogart, GA, 1989) set of programs. The reaction of AXCP with NO at −20 °C was performed in a cryosolvent consisting of a 1:4 mixture (v/v) of methanol and aqueous buffer. A 3:2 methanol−buffer mixture was used for lower temperatures. Time-resolved absorption changes were measured using a Hi-Tech SF-3 L low-temperature stopped-flow instrument (Hi-Tech Scientific, Salisbury, UK) equipped with a J&M TIDAS 16/300-1100 diode array spectrophotometer (J&M, Aalen, Germany). The optical cell had a light path of 1.0 cm and was connected to the spectrophotometer unit with flexible light guides. The mixing chamber and drive syringes (5-mL capacity) were immersed in an ethanol bath that was cooled by liquid N_2 evaporation. A Pt resistance thermometer and PID temperature-controlled thyristor heating unit (both Hi-Tech) were used to maintain the temperature at ±0.1 °C. Complete spectra were collected between 372 and 732 nm with the integrated J&M software Kinspec 2.30.

Heme−NO Dissociation Kinetics. UV−vis spectra and kinetic traces for the determination of the back rate constant, k_{6off}, at 25.0 °C were measured using a Cary 50 spectrophotometer equipped with a thermostatted cell holder. The 6c-NO−AXCP complex was prepared inside an anaerobic cuvette at 25 °C by titrating ferrous AXCP (~3 μM in heme) with NO-saturated buffer (to a 2−3-fold excess), as previously described.[14] Under these conditions, AXCP samples containing significant proportions of 6c-NO heme (λ_{max} 415 nm) are stable for tens of seconds. The release of NO from heme was initiated by adding excess dithionite (as NO scavenger) to a final concentration of 10−80 mM, according to previously described methods.[27] Values of k_{6off} were determined from single-exponential fits of time traces at 409.5 nm and represent the mean of five separate experiments. The choice of 409.5 nm as the monitoring wavelength (an isosbestic point of the 5c-Fe^{2+} and 5c-NO absorbance spectra (see Figure 1A)) avoids off-rate contributions from any 5c-NO complex present in the sample. To confirm that the back reaction, k_{6off}, is indeed slow, additional measurements of k_{6off} were carried out in the presence of 0.5−3 mM Fe^{II}(edta), which has a very high second-order rate constant for reaction with NO, viz., ~1 × 10^8 M^{-1} s^{-1} at pH 5 and 25 °C.[28] Off-rate determinations using Fe^{II}(edta) were performed using a Shimadzu UV-2100 spectrophotometer equipped with a thermostatted cell compartment CPS-260. A lower temperature (10.0 °C) was used to minimize the conversion of 6c-NO to proximal 5c-NO that might interfere with the back reaction.

Results and Discussion

Kinetic Measurements of AXCP−NO Binding Reactions. Whereas NO binding to most ferrous heme proteins is typically too fast to be measured by rapid mixing techniques, the relatively slow reaction of NO with ferrous AXCP is readily monitored on the stopped-flow time scale. Previous stopped-flow measurements of NO binding to AXCP, monitored by FTIR[13] and single-wavelength UV−vis absorbance,[14] identified a 6c-NO intermediate during 5c-NO formation. In this study, stopped-flow UV−vis absorbance spectra were recorded to characterize the heme chromophores involved. A typical series of time-resolved optical absorption spectra are shown in Figure 1A. In agreement with previous observations, the reaction is biphasic: pentacoordinate ferrous heme (λ_{max} 425, 435 (s) nm) forms a 6c-NO intermediate (λ_{max} 416 nm) which then converts to a 5c-NO product (λ_{max} 395 nm). Singular value decomposition of the time-resolved spectra is consistent with the three spectrally distinct heme species outlined above (Figure 1B, Scheme 1).

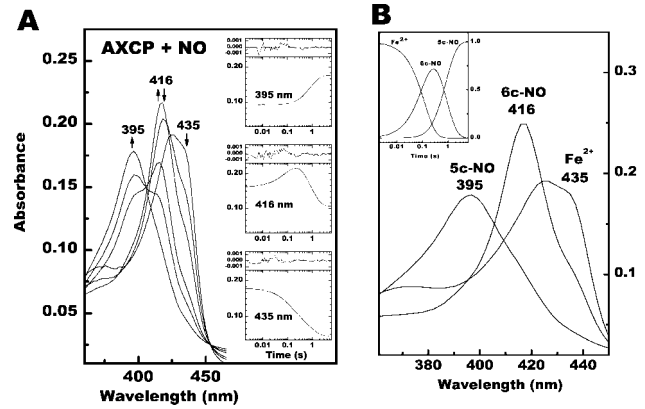

Figure 1. (A) Absorption spectra for the reaction of ferrous AXCP with 0.2 mM NO (ambient pressure, 25.0 °C) recorded at 0.0006, 0.072, 0.19, 0.79, 1.3, and 4.5 s. Reaction solutions contained 50 mM CHES buffer (pH 8.9) and 0.10 M NaCl. Insets show time courses at 395, 416, and 435 nm, along with kinetic fits and residuals for an A → B → C reaction. (B) Calculated absorption spectra of the kinetic components of the reaction, along with their time-dependent concentrations (inset).

Global kinetic analysis using an A → B → C model yields pseudo-first-order rate constants, $k_{obs(A)}$ and $k_{obs(B)}$, for the first and second phases, respectively. As observed previously, both $k_{obs(A)}$ and $k_{obs(B)}$ exhibit a linear dependence on NO concentration (Table 1, Figure 2) consistent with the proposed mechanism in Scheme 1. For reactions at 25.0 °C, plots of $k_{obs(A)}$ and $k_{obs(B)}$ versus NO concentration yield bimolecular rate constants k_{6on} (4.3 × 10^4 M^{-1} s^{-1}) and k_{6-5} (1.1 × 10^4 M^{-1} s^{-1}), respectively, in good agreement with previous stopped-flow (single-wavelength)[13,14] and flash photolysis experiments[15] (Tables 1 and 3). The almost zero intercepts found for the plots of $k_{obs(A)}$ and $k_{obs(B)}$ versus NO concentration indicate that the back reaction rates of both phases (Scheme 1) are relatively slow. Indeed, direct measurement of the NO dissociation rate of the 6c-NO intermediate (k_{6off}) using dithionite as NO-scavenger yields $k_{6off} = (6.0 \pm 0.5) \times 10^{-3}$ s^{-1} at 25.0 °C (Figure 3). The off rate constant is independent of the dithionite concentration (10−80 mM), consistent with k_{6off} being the rate-determining step. A somewhat lower off rate constant (~1.0 × 10^{-3} s^{-1}) is observed at 10 °C with Fe^{II}(edta) (0.5−3 mM) as the NO-scavenger, consistent with a decrease in the off rate as the temperature is lowered.

Activation Parameters for NO Binding to AXCP. Values of $\Delta S^{\ddagger}$ and $\Delta H^{\ddagger}$ for NO binding to AXCP were obtained by measuring k_{6on} and k_{6-5} as a function of temperature (10.0−30.0 °C). At each reaction temperature, k_{6on} and k_{6-5} were calculated from the NO-dependence of $k_{obs(A)}$ and $k_{obs(B)}$, respectively (Table

(25) van Eldik, R.; Palmer, D. A.; Schmidt, R.; Kelm, H. *Inorg. Chim. Acta* **1981**, *50*, 131–135.
(26) van Eldik, R.; Gaede, W.; Wieland, S.; Kraft, J.; Spitzer, M.; Palmer, D. A. *Rev. Sci. Instrum.* **1993**, *64*, 1355–1357.
(27) Kharitonov, V. G.; Sharma, V. S.; Magde, D.; Koesling, D. *Biochemistry* **1997**, *36*, 6814–6818.
(28) Schneppensieper, T.; Wanat, A.; Stochel, G.; Goldstein, S.; Meyerstein, D.; van Eldik, R. *Eur. J. Chem.* **2001**, 2317–2325.

Table 1. Pseudo-First-Order Rate Constants for the First ($k_{obs(A)}$) and Second ($k_{obs(B)}$) Reactions of NO with AXCP as a Function of [NO] and Temperature[a]

T (°C)	[NO] (mM)	$k_{obs(A)}$ (s^{-1})	$10^{-4}k_{6on}$ (M^{-1} s^{-1})	$k_{obs(B)}$ (s^{-1})	$10^{-4}k_{6-5}$ (M^{-1} s^{-1})
10.0	40	0.505		0.0653	
	66	1.07		0.151	
	79	1.15	1.49 ± 0.04	0.167	0.194 ± 0.009
	129	2.03		0.274	
	190	2.76		0.343	
15.0	40	0.774		0.120	
	66	1.36		0.227	
	79	1.500	2.21 ± 0.07	0.254	0.332 ± 0.005
	129	2.78		0.447	
	190	4.39		0.621	
20.0	40	1.20		0.241	
	66	2.24		0.416	
	79	2.69	3.29 ± 0.07	0.548	0.633 ± 0.012
	129	4.26		0.835	
	190	6.19		1.17	
25.0	40	1.65		0.412	
	66	2.69		0.636	
	79	3.37	4.33 ± 0.04	0.775	1.14 ± 0.04
	129	5.64		1.46	
	190	8.30		2.27	
30.0	40	2.45		0.644	
	66	3.99		1.18	
	79	5.08	5.71 ± 0.19	1.57	1.92 ± 0.04
	129	7.76		2.61	
	190	10.2		3.57	

[a] Buffer conditions are as described in Figure 1.

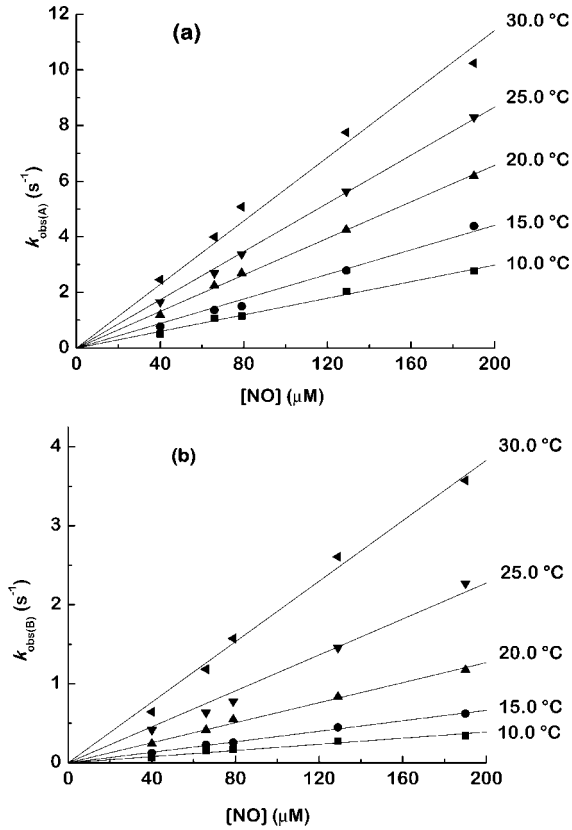

Figure 2. Plots of k_{obs} versus NO concentration as a function of temperature for the reaction of NO with AXCP: (a) first reaction and (b) second reaction.

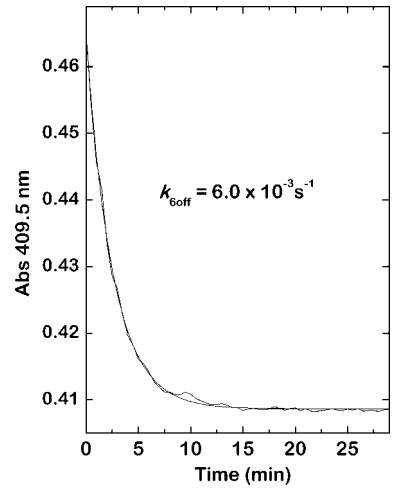

Figure 3. Reaction time course (409.5 nm) for the release of NO from 6c-NO−AXCP at 25.0 °C in the presence of 10 mM sodium dithionite, overlaid with a single -exponential fit. Buffer conditions are as described in Figure 1.

1, Figure 2). Eyring plots (Figure 4) yield $\Delta S^{\ddagger} = -3 \pm 7$ J K^{-1} mol^{-1} and $\Delta H^{\ddagger} = 46 \pm 2$ kJ mol^{-1} for the first NO-binding step (k_{6on}), together with $\Delta S^{\ddagger} = +103 \pm 5$ J K^{-1} mol^{-1} and $\Delta H^{\ddagger} = 81 \pm 2$ kJ mol^{-1} for the second NO-binding step (k_{6-5}). Volumes of activation, $\Delta V^{\ddagger}$, were determined from the dependence of k_{6on} and k_{6-5} on hydrostatic pressure (0−130 MPa). Bimolecular rate constants were calculated from reactions conducted in the presence of 0.1 mM NO at 25.0 °C, assuming a linear dependence of $k_{obs(A)}$ and $k_{obs(B)}$ on NO concentration and negligible intercepts for these plots. Both NO-binding reactions occur more slowly at higher pressure, with the second reaction (k_{6-5}) more sensitive to pressure than the first (k_{6on}) (Figure 5). Plots of ln(k) versus pressure (Figure 5) yield $\Delta V^{\ddagger} = +14.1 \pm 0.7$ cm^3 mol^{-1} for k_{6on} and $\Delta V^{\ddagger} = +24.1 \pm 0.3$ cm^3 mol^{-1} for k_{6-5}. Varying the temperature from 25 to 15 °C had no apparent effect on the $\Delta V^{\ddagger}$ values (Table 2). Several series of experiments were performed to check the reproducibility of the data. The results in Table 2 also demonstrate that the reported volumes of activation are not temperature-sensitive in the range 10−25 °C. Activation parameters and rate constants for NO-binding reactions of AXCP and other heme systems are summarized in Table 3.

Mechanism of Distal NO Binding. Heme−nitrosyl formation in ferrous AXCP begins with NO binding to the empty distal site of the ferrous heme to generate a 6c-NO complex. In principle, a rate-determining step involving Fe^{2+}−NO bond formation, together with the high- to low-spin transition of the heme iron and its motion from "out-of-plane" to "in-plane", should make significantly negative contributions to the overall $\Delta S^{\ddagger}$ and $\Delta V^{\ddagger}$ values for 6c-NO formation. However, the observation of a near-zero $\Delta S^{\ddagger}$ and significantly positive $\Delta V^{\ddagger}$ value (+14.1 cm^3 mol^{-1}) suggests that factors other than Fe^{2+}−NO bond formation contribute to the rate-determining step.

The rate of distal NO binding to AXCP is unusually low for a pentacoordinate ferrous heme ($k_{6on} = 4.3 \times 10^4$ M^{-1} s^{-1}), some 3 orders of magnitude lower than for ferrous myoglobin (Table 3). In fact, the k_{6on} value is similar to that for NO binding to ferric myoglobin (Table 3), where the positive $\Delta S^{\ddagger}$ and $\Delta V^{\ddagger}$ values are attributed to a rate-determining step involving the release of a distal aqua ligand prior to Fe^{3+}−NO bond

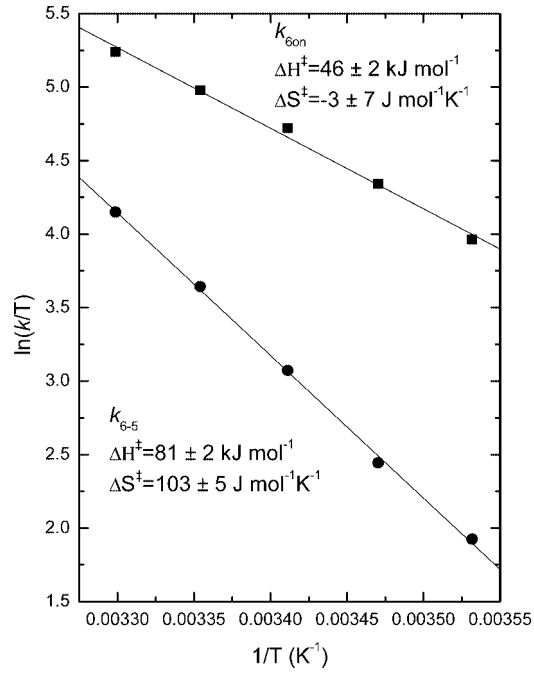

Figure 4. Eyring plots of $\ln(k_{6on}/T)$ and $\ln(k_{6-5}/T)$ versus $1/T$ for NO binding to AXCP. Buffer conditions are as described in Figure 1.

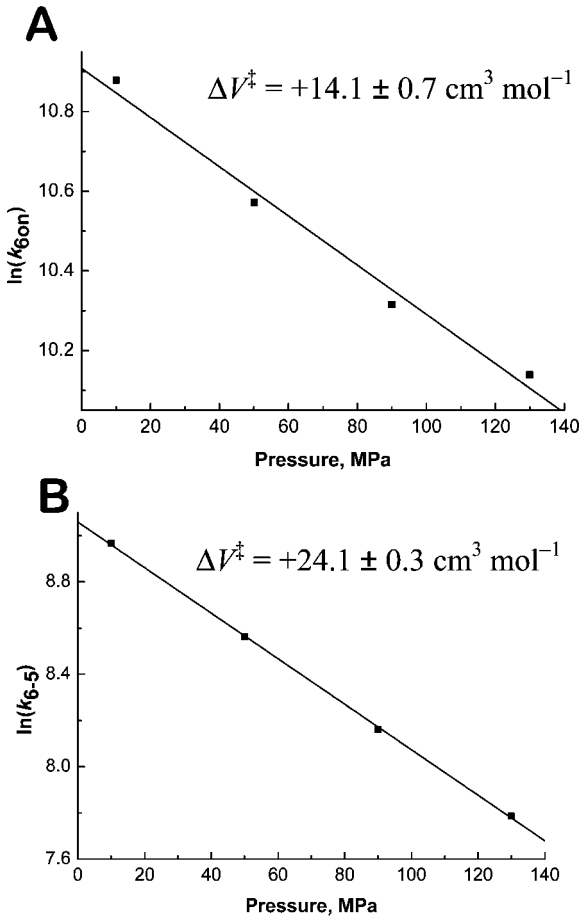

Figure 5. Representative plots of (A) $\ln(k_{6on})$ versus hydrostatic pressure and (B) $\ln(k_{6-5})$ versus hydrostatic pressure for NO binding to AXCP at 25.0 °C. Buffer conditions are as described in Figure 1.

formation.[29] However, unlike ferric myoglobin, ferrous AXCP does not contain any solvent molecules within the distal pocket.[10] Rather, it is likely that the AXCP protein architecture governs distal NO binding, such that the rate-determining step involves ligand migration to the heme. The distal pocket of AXCP is buried within the protein interior, and access of ligands to the heme face is hindered by the Leu 16 residue within the crowded distal pocket. A comparison of the AXCP ferrous and 6c-CO crystal structures reveals that the $C_\alpha-C_\beta$ bond of Leu 16 rotates by 134° to accommodate the distal CO ligand.[10] Although the crystal structure of the transient 6c-NO complex of AXCP has yet to be determined, it is expected that NO binding to the distal heme face should also be accompanied by a movement of Leu 16, similar to that of the 6c-CO complex.

Table 2. Calculated $\Delta V^{\ddagger}$ Values from Several Series of Experiments for NO Binding to Ferrous AXCP at 15.0 and 25.0 °C[a]

	$\Delta V^{\ddagger}$ (cm^3 mol^{-1})	
T (°C)	first reaction (k_{6on})	second reaction (k_{6-5})
15.0	12.2 ± 0.4	24.4 ± 2.9
	13.0 ± 0.1	24.1 ± 4.3
	13.5 ± 0.4	26.7 ± 1.2
	14.4 ± 1.6	24.1 ± 1.7
25.0	14.1 ± 0.7	24.1 ± 0.3
	12.4 ± 0.9	22.9 ± 0.6
	14.5 ± 0.1	
	12.2 ± 0.9	

[a] Buffer conditions are as described in Figure 1.

In view of the distal protein environment of AXCP, the positive $\Delta V^{\ddagger}$ value (+14.1 cm^3 mol^{-1}) can be explained in terms of the effect of pressure on the volume of the distal heme pocket. Namely, increased pressure will compress the volume of the AXCP distal heme cavity, hindering the Leu 16 conformation change and increasing the energy barrier for NO migration to the distal coordination site. As a result, increased pressure will decelerate the NO-binding reaction, and the contribution of the NO migration process to the rate-limiting step will cause the activation volume for this reaction to be significantly positive. A similar effect of pressure, ascribed to ligand migration processes, has been observed in high-pressure studies of small-molecule binding to ferrous myoglobin.[30] Overall, the activation parameters for distal NO binding to ferrous AXCP support the hypothesis that this process is governed by steric hindrance within the crowded distal pocket.[31] Steric hindrance to distal heme coordination is also consistent with the low rate of CO binding to AXCP (92 M^{-1} s^{-1}).[32] In addition, ferric AXCP has been shown to react very slowly with NO (several hours) to form a ferrous nitrosyl product without any detectable ferric nitrosyl species.[33] The absence of a detectable ferric nitrosyl complex is indicative of a slow heme−NO binding step (due to steric hindrance), followed by relatively rapid reductive nitrosylation.

Mechanism of 6c-NO to 5c-NO Conversion. Formation of the distal 6c-NO−AXCP species is followed by its conversion to a

(29) Laverman, L. E.; Wanat, A.; Oszajca, J.; Stochel, G.; Ford, P. C.; van Eldik, R. *J. Am. Chem. Soc.* **2001**, *123*, 285–293.
(30) Uchida, T.; Ishimori, K.; Morishima, I. *J. Biol. Chem.* **2000**, *275*, 30309–30316.
(31) Andrew, C. R.; Kemper, L. J.; Busche, T. L.; Tiwari, A. M.; Kecskes, M. C.; Stafford, J. M.; Croft, L. C.; Lu, S.; Moënne-Loccoz, P.; Huston, W.; Moir, J. W. B.; Eady, R. R. *Biochemistry* **2005**, *44*, 8664–8672.
(32) Cusanovich, M. A.; Gibson, Q. H. *J. Biol. Chem.* **1973**, *248*, 822–834.
(33) Yoshimura, T.; Suzuki, S.; Nakahara, A.; Iwasaki, H.; Masuko, M.; Matsubara, T. *Biochemistry* **1986**, *25*, 2436–22442.

Table 3. Rate Constants and Activation Parameters for NO Binding to Heme Proteins[a]

	k (M^{-1} s^{-1})	$\Delta H^{\ddagger}$ (kJ mol^{-1})	$\Delta S^{\ddagger}$ (J mol^{-1} K^{-1})	$\Delta V^{\ddagger}$ (cm^3 mol^{-1})	ref
AXCP (Fe^{2+})					
(k_{6on})	4.3×10^4	46 ± 2	-3 ± 7	$+14.1 \pm 0.7$	this work
	4.4×10^4	nd[b]	nd	nd	14
(k_{6-5})	1.1×10^4	81 ± 2	$+103 \pm 5$	$+24.1 \pm 0.3$	this work
	8.7×10^3	nd	nd	nd	14
sGC (Fe^{2+})[c]					
(k_{6on})	$>1.4 \times 10^8$	nd	nd	nd	18
(k_{6-5})	2.4×10^5	nd	nd	nd	18
Fe^{2+}(TPP)[d]	5.2×10^9	2.6	-51	nd	45
Mb (Fe^{2+})[e]	1.7×10^7	nd	nd	nd	46
metMb (Fe^{3+})[f]	4.8×10^4	71 ± 2	$+82 \pm 7$	$+21 \pm 1$	29
$P450_{cam}$ (Fe^{3+})[g]	3.2×10^5	92 ± 1	$+169 \pm 4$	$+28 \pm 2$	41

[a] Data obtained at ambient pressure and 25.0 °C unless otherwise indicated. [b] nd, not determined. [c] sGC, soluble guanylate cyclase ($\alpha_1\beta_1$ isoform) from bovine lung, data obtained at 4.0 °C. [d] Fe^{2+}(TPP), ferrous complex of *meso*-tetraphenylporphyrin. [e] Mb, sperm whale ferrous myoglobin, data obtained at 20.0 °C. [f] metMb, horse heart ferric myoglobin. [g] $P450_{cam}$, ferric cytochrome P450 from *Pseudomonas putida*.

low-spin 5c-NO product in which NO resides on the proximal heme face at the site originally occupied by the His ligand (Scheme 1). The NO-dependence of the 6c-NO → 5c-NO conversion, together with the proximal coordination of the 5c-NO end product, has led to the suggestion that proximal NO binding to AXCP occurs via a putative dinitrosyl intermediate.[11,14] A similar mechanism has been proposed for the formation of the 5c-NO complex of the $\alpha_1\beta_1$ isoform of the mammalian NO-sensor, sGC.[20−22] For both AXCP and sGC, theoretical studies suggest that a dinitrosyl intermediate is a plausible species in the 5c-NO formation mechanism.[16,17] The reaction of AXCP with stoichiometric NO (1:1 ratio of NO to heme) also leads to a 5c-NO end product via a transient 6c-NO intermediate,[34] consistent with a mechanism requiring one net NO molecule for the overall reaction (such as in Scheme 1). When the NO concentration is less than that of the AXCP heme, the coordination number of the heme−nitrosyl complex is seen to depend on the temperature. Only the 6c-NO species was observed in the present study when substoichiometric NO (0.8: 1 ratio of NO to heme) was added to AXCP at 10 °C (no 5c-NO species was detected over a period of 40 min). On the other hand, 6c-NO → 5c-NO conversion is observed when substoichiometric NO is added to AXCP at a higher temperature of 25 °C.[14,34] The nature of the 5c-NO AXCP complex (proximal or distal) formed with substoichiometric NO has yet to be determined, although it is possible that dinitrosyl (and hence proximal 5c-NO) formation might occur, given that the magnitude of k_{6-5} is relatively close to that of k_{6on}, particularly at higher temperature (k_{6on}:k_{6-5} ~3.8 at 25 °C (Table 1)).

Due to their inherent instability, only a relatively few metalloporphyrin-based dinitrosyl complexes have been reported, including tetrapyrrole complexes of Ru and Fe.[35−38] A Co−dinitrosyl complex has also been proposed as a reaction intermediate.[39] According to the literature, formation of dinitrosyl ferrous heme complexes at room temperature is thermodynamically unfavorable.[36−40] For example, the equilibrium constant, $K_{(NO)_2}$, for the formation of the dinitrosyl model porphyrin, Fe(TmTP)$(NO)_2$ (eq 1),

$$Fe^{II}(TmTP)(NO) + NO \rightleftarrows Fe^{II}(TmTP)(NO)_2 \qquad (1)$$

was determined to be 23 M^{-1} at 253 K.[36] From the temperature dependence of $K_{(NO)_2}$, it can be estimated that at room temperature (298 K) this constant is ~2.1 M^{-1}. Therefore, we conclude that, if the 6c-NO → 5c-NO conversion in AXCP were to occur via a dinitrosyl intermediate, the detection of such an intermediate should not be possible at room temperature. Indeed, neither the present room-temperature stopped-flow UV−vis spectra (Figure 1) nor the previous stopped-flow FTIR spectra[13] show any evidence of a spectrally distinct dinitrosyl species. Additional low-temperature stopped-flow measurements carried out at −20 °C, using a methanol/water cryosolvent, yielded heme absorption spectra similar to those at room temperature, with no detectable dinitrosyl intermediate (data not shown). At temperatures below −20 °C, significant perturbations in the ferrous AXCP absorption indicated a disruption of the protein structure due to the cryosolvent.

Mechanism of Dinitrosyl Formation. The fact that the dinitrosyl intermediate is not directly observed can be accounted for not only in terms of an unfavorable equilibrium for the formation of this species, but also in terms of the rapid decomposition of the dinitrosyl complex to the 5c-NO final product. This means that formation of the dinitrosyl intermediate should be the rate-determining step in Scheme 1, whereas decomposition of the dinitrosyl intermediate to the 5c-NO product must be relatively rapid, such that the dinitrosyl species is not observed under the selected reaction conditions. In this case, the fast reaction following the rate-determining step should not contribute to the activation parameters determined for the overall 6c-NO → 5c-NO conversion. On this basis, the activation parameters for the second reaction (k_{6-5}) should describe the formation of the dinitrosyl intermediate that involves replacement of the proximal His ligand.

Scheme 2 shows two possible ways for a 6c-NO complex to form a dinitrosyl intermediate. Pathway (i) shows dinitrosyl formation via a limiting dissociative mechanism in which the His ligand of the 6c-NO species is released to form a distal 5c-NO intermediate prior to attack of the second NO molecule on the proximal heme face. In this case, large and positive values of $\Delta S^{\ddagger}$ and $\Delta V^{\ddagger}$ are expected due to the Fe−His bond cleavage that accompanies the formation of the transition state. The other route (pathway (ii) in Scheme 2) shows a concerted dissociative

(34) Barbieri, S.; Murphy, L. M.; Sawers, R. G.; Eady, R. R.; Hasnain, S. S. *J. Biol. Inorg. Chem* **2008**, *13*, 531–540.
(35) Wayland, B. B.; Olson, L. W. *J. Am. Chem. Soc.* **1974**, *96*, 6037–6041.
(36) Lorkovic, I.; Ford, P. C. *J. Am. Chem. Soc.* **2000**, *122*, 6516–6517.
(37) Patterson, J. C.; Lorkovic, I. M.; Ford, P. C. *Inorg. Chem.* **2003**, *42*, 4902–4908.
(38) Lim, M. D.; Lorkovic, I. M.; Ford, P. C. *J. Inorg. Biochem.* **2005**, *99*, 151–165.
(39) Franke, A.; Roncaroli, F.; van Eldik, R. *Eur. J. Inorg. Chem.* **2007**, 773–798.
(40) Lorkovic, I. M.; Ford, P. C. *Inorg. Chem.* **2000**, *39*, 632–633.

Scheme 2. Proposed Pathways for the Formation of a 6c-$(NO)_2$ Heme Complex from a 6c-NO Heme Complex, Including the Transition States Involved

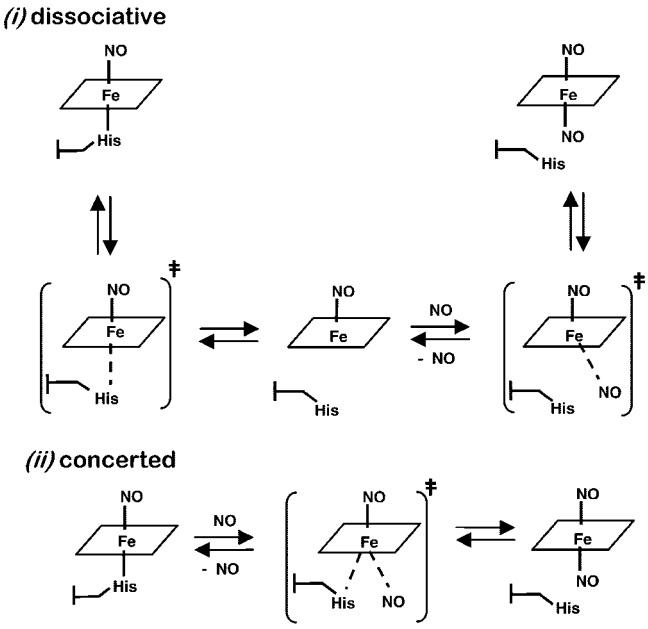

Scheme 3. Summary of the Essential Reaction Steps in the Limiting Dissociative Mechanism

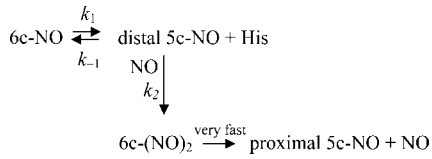

interchange mechanism (I_d) in which both NO and the proximal His ligand are partially bound to the metal center in the transition state. In this case, the values of activation entropy and activation volume are expected to be significantly smaller than those for a limiting dissociative mechanism. On this basis, the large and positive values of $\Delta S^{\ddagger}$ and $\Delta V^{\ddagger}$ determined in the present study for the 6c-NO to proximal 5c-NO transition strongly support a limiting dissociative mechanism for dinitrosyl formation (pathway (i) in Scheme 2). It should be noted that transition states are included in this scheme to emphasize the fact that the limiting dissociative mechanism involves two subsequent reaction steps with two transition states, whereas the concerted (or interchange) mechanism is a one-step process with a single transition state.

According to the mechanism described above, the essential steps describing the 6c-NO to proximal 5c-NO conversion are shown in Scheme 3. This scheme is useful since it deals specifically with the elementary reaction steps and rate constants that define the observed rate constant for the second reaction with NO, i.e., $k_{obs(B)}$. Assuming that the decomposition of the dinitrosyl intermediate to proximal 5c-NO is very fast, it follows that the k_2 reaction in Scheme 3 is essentially irreversible (i.e., the back reaction, k_{-2}, is negligible). In this case, the expression for the observed first-order rate constant for the conversion of 6c-NO to proximal 5c-NO ($k_{obs(B)}$) is given by eq 2.

$$k_{obs(B)} = \frac{k_1 k_2[NO]}{k_{-1} + k_2[NO]} \qquad (2)$$

In light of the linear dependence of $k_{obs(B)}$ on the NO concentration, i.e., $k_{-1} \gg k_2[NO]$, the expression for $k_{obs(B)}$ can be simplified to eq 3.

$$k_{obs(B)} = \frac{k_1 k_2}{k_{-1}}[NO] = K_1 k_2[NO] \qquad K_1 = k_1/k_{-1} \quad (3)$$

According to eq 3, $k_{obs(B)}$ depends on the rate of His dissociation (k_1 in Scheme 3), i.e., the rate-determining step that dominates the activation parameters. However, $k_{obs(B)}$ is also seen to depend on the rate constant for proximal NO binding to the 5c-NO distal intermediate (k_2 in Scheme 3). This explains why there is an observed [NO]-dependence for this reaction, even though Fe---His dissociation is the slowest step of the overall reaction and the one that dominates the activation parameters. However, the rate of proximal NO binding also affects $k_{obs(B)}$ since it is this reaction that competes with His reattachment (k_{-1}), thereby trapping the distal 5c-NO intermediate to form the obligatory dinitrosyl species required for proximal 5c-NO formation.

Accordingly, the second-order rate constant determined for the conversion of 6c-NO to proximal 5c-NO is represented by $k_{6-5} = k_1k_2/k_{-1} = K_1k_2$. In this context, the activation parameters determined from the temperature and pressure dependence of k_{6-5} reflect the following sums (eqs 4 − 6):

$$\Delta H^{\ddagger}_{6-5} = \Delta H^{\ddagger}_1 + \Delta H^{\ddagger}_2 - \Delta H^{\ddagger}_{-1} \qquad (4)$$

$$\Delta S^{\ddagger}_{6-5} = \Delta S^{\ddagger}_1 + \Delta S^{\ddagger}_2 - \Delta S^{\ddagger}_{-1} \qquad (5)$$

$$\Delta V^{\ddagger}_{6-5} = \Delta V^{\ddagger}_1 + \Delta V^{\ddagger}_2 - \Delta V^{\ddagger}_{-1} \qquad (6)$$

Taking into account that both the reactions k_{-1} and k_2 involve ligand binding (His and NO, respectively) to the unsaturated distal 5c-NO, the contributions $\Delta H^{\ddagger}_2 - \Delta H^{\ddagger}_{-1}$, $\Delta S^{\ddagger}_2 - \Delta S^{\ddagger}_{-1}$, and $\Delta V^{\ddagger}_2 - \Delta V^{\ddagger}_{-1}$ to the overall expressions for activation parameters of k_{6-5} should be negligible. This means that the contribution coming from reaction k_1 involving dissociation of His to form the distal 5c-NO intermediate dominates the overall activation parameters. Therefore, the substantially positive values of $\Delta S^{\ddagger}_{6-5}$ (+103 J K^{-1} mol^{-1}) and $\Delta V^{\ddagger}_{6-5}$ (+24.1 cm^3 mol^{-1}) found in the present study for the conversion of 6c-NO to proximal 5c-NO should be accounted for in terms of the scission of the Fe−His bond, as well as the considerable movement (rotation) of the His 120 ligand to its displaced conformation within the AXCP proximal heme pocket.[10] Precedence for large positive $\Delta S^{\ddagger}$ and $\Delta V^{\ddagger}$ values in heme−NO binding reactions exists for metMb[29] and the resting state of cytochrome $P450_{cam}$[41] (Table 3). In these proteins, the large positive $\Delta S^{\ddagger}$ and $\Delta V^{\ddagger}$ values for NO binding (Table 3) were ascribed to a limiting dissociative ligand substitution mechanism in which the activation parameters are dominated by the dissociation of a heme aqua ligand, accompanied by structural rearrangements in the heme pocket.

Determinants of Proximal 5c-NO Formation. It follows that a dissociative mechanism for dinitrosyl formation implies that the rate-limiting step of k_{6-5} is the spontaneous release of the His ligand from the 6c-NO complex to form a distal 5c-NO intermediate. Structural characterization of 6c-NO ferrous nitrosyl model porphyrins has shown that the NO ligand in $\{FeNO\}^7$ systems exerts a strong *trans* influence, which results in an unusually long bond *trans* to the nitrosyl ligand.[42] Accordingly, the His ligand of the 6c-NO AXCP species may be relatively weakly bound and labile. However, in the 5c-Fe^{2+}

state at least, AXCP has a relatively high Fe−His stretching frequency (231 cm^{-1}),[12] which is significantly higher than the proposed limit (210 cm^{-1}) above which heme proteins are expected to retain their His ligands to yield stable 6c-NO complexes.[43] The apparently anomalous behavior of AXCP may be due to the influence of the surrounding protein matrix on His ligand release. Indeed, recent computational studies by Martí et al. suggest that the Fe−His bond of AXCP breaks because of a local energy minimum for the unbound conformation of the proximal His 120 ligand.[17]

Although the rate-determining step of dinitrosyl formation is the release of the His ligand (Scheme 2, pathway (i)), dinitrosyl formation also depends on the rate of proximal NO binding to the distal 5c-NO intermediate (eq 3). For the distal 5c-NO intermediate to convert to the dinitrosyl complex, proximal NO binding from solution (k_2) must be fast enough to compete with His ligand reattachment (k_{-1}). We propose that the key to dinitrosyl formation in AXCP is the solvent exposure of the proximal heme face that enables proximal NO binding to trap at least some dinitrosyl species before the His ligand can reattach.

The lack of an observable dinitrosyl intermediate is consistent with its expected rapid rate of decay to the 5c-NO product. We attribute the exclusive proximal heme−NO geometry of the 5c-NO product to preferential loss of distal NO from the dinitrosyl intermediate due to steric hindrance from Leu 16. This is in line with previous studies suggesting that steric accessibility governs heme−NO geometry in cytochromes *c*′,[31] as well as calculations that indicate a lower dissociation energy barrier for the distal (rather than proximal) NO ligand of the AXCP dinitrosyl intermediate.[17] It is also noted the somewhat higher k_{6off} value for 6c-NO−AXCP (6.0×10^{-3} s^{-1}) relative to other 6c-NO−heme proteins, e.g., myoglobin (3.4×10^{-4} s^{-1}),[44] could arise from steric destabilization of the distal NO ligand. Another important consequence of distal heme steric hindrance in AXCP is that it causes dinitrosyl decomposition to the proximal 5c-NO product to be essentially irreversible (Scheme 3). Therefore, even if the equilibrium between the 6c-NO and distal 5c-NO intermediate (Scheme 3) lies far to the left (due, for example, to unfavorable His dissociation and/or rapid His reattachment), all of the sample will eventually convert to the proximal 5c-NO product as long as some dinitrosyl species is formed. This may also help to explain why AXCP is able to form a 5c-NO product despite its apparently strong Fe−His bond.

In summary, activation parameters determined for NO binding to AXCP provide detailed information about the mechanism of proximal 5c-NO formation, including the role of the dinitrosyl intermediate and the influence of the proximal and distal heme environments. Values of $\Delta S^{\ddagger}$ and $\Delta V^{\ddagger}$ for the 6c-NO formation reaction (k_{6on}) are consistent with significant steric hindrance to distal NO binding from the Leu 16 residue. In the subsequent distal (6c-NO) to proximal (5c-NO) conversion, large positive $\Delta S^{\ddagger}$ and $\Delta V^{\ddagger}$ values support a limiting dissociative mechanism in which the rate-limiting step for dinitrosyl formation involves Fe−His bond scission to form a distal 5c-NO intermediate (Scheme 2, pathway (i)). Rapid proximal NO binding to this distal 5c-NO species leads to a dinitrosyl intermediate, which then rapidly decomposes to the 5c-NO product by selective dissociation of the distal NO. An alternative pathway for dinitrosyl formation, involving the concerted replacement of the proximal His ligand by an incoming NO (Scheme 2, pathway (ii)), is ruled out. The major requirements for proximal 5c-NO formation in AXCP are seen to be as follows: (i) spontaneous Fe−His bond cleavage in the 6c-NO complex (facilitated by a *trans* influence), (ii) formation of a dinitrosyl intermediate (facilitated by rapid proximal NO binding due to the solvent-exposed proximal heme), and (iii) decomposition of the dinitrosyl intermediate to the proximal 5c-NO product (facilitated by steric hindrance to distal heme coordination). The ability of AXCP to alternate between distal heme−NO interactions (disfavored by steric hindrance) and proximal NO binding (favored by solvent exposure) is key to its novel proximal NO-binding ability. While it is recognized that AXCP differs in many respects from the heme−NO sensor, sGC, the possibility remains that proximal heme−NO binding, via a dinitrosyl intermediate, could occur in sGC. Future crystallographic characterizations of the sGC heme domain should reveal whether any of the structural features associated with proximal NO binding in AXCP are present in sGC.

Acknowledgment. The authors gratefully acknowledge financial support from National Science Foundation grants MCB-0417152 and MCB-0745035 (to C.R.A.) and Deutsche Forschungsgemeinschaft grant SFB 583 "Redox-active metal complexes" (to R.v.E.). C.R.A. thanks Lenord Kemper, Arianne Tiwari, Alison McKay, and Amy Servid for help with preliminary data.

JA809587Q

(41) Franke, A.; Stochel, G.; Jung, C.; van Eldik, R. *J. Am. Chem. Soc.* **2004**, *126*, 4181–4191.
(42) Scheidt, W. R.; Ellison, M. K. *Acc. Chem. Res.* **1999**, *32*, 350–359.
(43) Schelvis, J. P. M.; Seibold, S. A.; Cerda, J. F.; Garavito, R. M.; Babcock, G. T. *J. Phys. Chem. B* **2000**, *104*, 10844–10850.
(44) Decatur, S. M.; Franzen, S.; DePillis, G. D.; Dyer, R. B.; Woodruff, W. H.; Boxer, S. G. *Biochemistry* **1996**, *35*, 4939–4944.
(45) Hoshino, M.; Laverman, L.; Ford, P. C. *Coord. Chem. Rev.* **1999**, *187*, 75–102.
(46) Moore, E. G.; Gibson, Q. H. *J. Biol. Chem.* **1976**, *251*, 2788–2794.